



HAL
open science

NMR relaxivity of coated and non-coated size-sorted maghemite nanoparticles

Jérôme Fresnais, Qianqian Ma, Linda Thai, Patrice Porion, Pierre Levitz, Anne-Laure Rollet

► **To cite this version:**

Jérôme Fresnais, Qianqian Ma, Linda Thai, Patrice Porion, Pierre Levitz, et al.. NMR relaxivity of coated and non-coated size-sorted maghemite nanoparticles. *Molecular Physics*, 2018, 117 (7-8), pp.990-999. 10.1080/00268976.2018.1527410 . hal-02173384

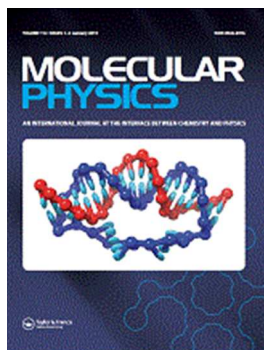
HAL Id: hal-02173384

<https://hal.science/hal-02173384>

Submitted on 21 Nov 2019

HAL is a multi-disciplinary open access archive for the deposit and dissemination of scientific research documents, whether they are published or not. The documents may come from teaching and research institutions in France or abroad, or from public or private research centers.

L'archive ouverte pluridisciplinaire **HAL**, est destinée au dépôt et à la diffusion de documents scientifiques de niveau recherche, publiés ou non, émanant des établissements d'enseignement et de recherche français ou étrangers, des laboratoires publics ou privés.



NMR relaxivity on coated and non-coated size-sorted maghemite nanoparticles

Journal:	<i>Molecular Physics</i>
Manuscript ID	TMPH-2018-0415
Manuscript Type:	Special Issue Paper
Date Submitted by the Author:	01-Jul-2018
Complete List of Authors:	Fresnais, Jerome; Physicochimie des Electrolytes et Nanosystemes Interfaciaux, Ma, QianQian; Physicochimie des Electrolytes et Nanosystemes Interfaciaux Thai, Linda; Physicochimie des Electrolytes et Nanosystemes Interfaciaux Porion, Patrice; ICMN Levitz, Pierre; Université Pierre et Marie Curie, Paris 6, Laboratoire PHENIX Rollet, Anne-Laure; University Pierre et Marie Curie,
Keywords:	maghemite nanoparticles, polymer coating, NMR relaxivity

SCHOLARONE™
Manuscripts

NMR relaxivity on coated and non-coated size-sorted maghemite nanoparticles

Jérôme Fresnais^{1*}, QianQian Ma¹, Linda Thai¹, Patrice Porion², Pierre Levitz¹
and Anne-Laure Rollet^{1*}

¹ Sorbonne Université, CNRS, Laboratoire de Physico-chimie des Electrolytes et Nanosystèmes Interfaciaux, PHENIX - UMR 8234, F-75252 Paris cedex 05, France.

² Interfaces, Confinement, Matériaux et Nanostructures, ICMN, UMR 7374, CNRS - Université d'Orléans, 45071 Orléans Cedex 02, France

* anne-laure.rollet@sorbonne-universite.fr ; jerome.fresnais@sorbonne-universite.fr

Statement of article significance

We investigate the NMR relaxation of iron oxide nanoparticles (MNPs). We sort by size MNPs to obtain numerous samples with diameter ranging from 4.5 to 12.5 nm with low polydispersity. We confirm that r_1 and r_2 NMR relaxivities increase with nanoparticle diameter. We also analyze the role of polydispersity for nanoparticles with the same mean size. Complementarily, we quantitatively investigate the role of coating on nanoparticles NMR relaxivity between bare and poly(sodium acrylate-co-maleate) coated nanoparticles (PAAMA). At last, we highlight that activation energy E_a decreases with nanoparticle diameter when determined from T_1 , but increases for T_2 determination.

1
2
3
4 **NMR relaxivity on coated and non-coated size-sorted maghemite**
5 **nanoparticles**
6
7

8 *Jérôme Fresnais^{1*}, QianQian Ma¹, Linda Thai¹, Patrice Porion², Pierre*
9 *Levitz¹ and Anne-Laure Rollet^{1*}*
10
11

12
13 ¹ *Sorbonne Université, CNRS, Laboratoire de Physico-chimie des Electrolytes et*
14 *Nanosystèmes Interfaciaux, PHENIX - UMR 8234, F-75252 Paris cedex 05, France.*
15
16

17 ² *Interfaces, Confinement, Matériaux et Nanostructures, ICMN, UMR 7374,*
18 *CNRS - Université d'Orléans, 45071 Orléans Cedex 02, France*
19
20
21
22

23
24 * anne-laure.rollet@sorbonne-universite.fr ; jerome.fresnais@sorbonne-universite.fr
25
26
27
28
29
30
31
32
33
34

35 ***Supplementary information***
36
37
38

39 SI-1 : scheme of size sorting process
40

41 Size sorting process was achieved to obtain the more monodispersed MNPs batches
42 (Fig. SI-1a). From the original unsorted ferrofluid, 8 secondary batches are produced.
43 Batches 2SC, 4SC, 5SC, 6SC, 7SC, and 8SC are sorted again to reach different sizes
44 with similar polydispersity. Sample 4SC9SC was sorted again to get 10.7 nm large
45 MNPs, compared to 11.2 for 4SC9SC sample.
46
47
48
49
50
51
52
53
54
55
56
57
58
59
60

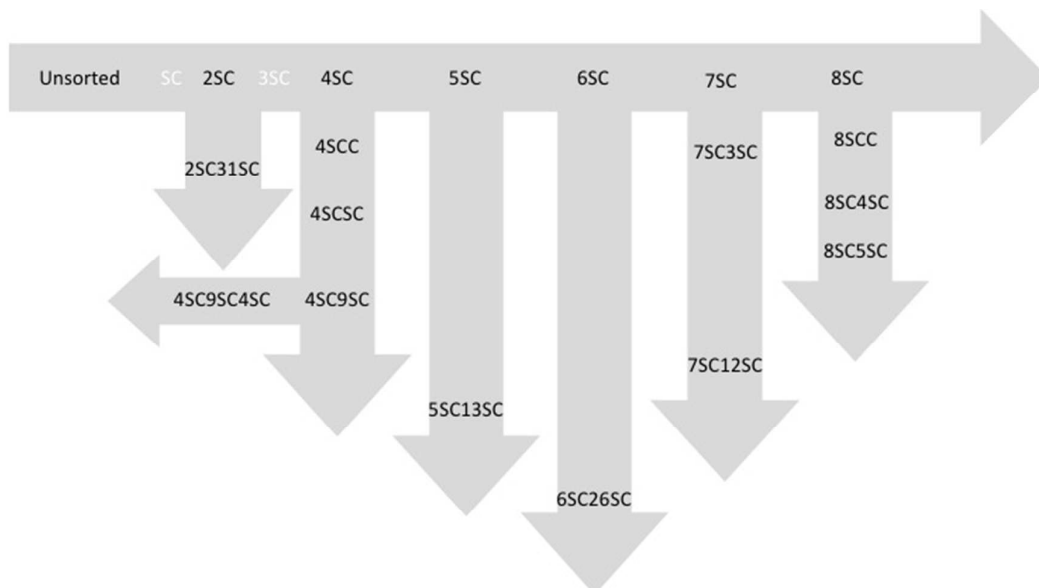


Figure SI-1a : size sorting process of the first batch used in this study.

To reach very small nanoparticles, another batch was used and sorted thoroughly to have two sample denoted YP6SC and YP 7SC with diameter of 5.6 nm and 4.5 nm, respectively (Fig. SI-1b).



Figure SI-1b : size sorting process of the first batch used in this study.

SI-2 : properties of MNPs synthesized in this study

Table 1 : VSM, TEM, diameters with their correlated polydispersity (lognormal distribution) and DLS diameter of samples used in this study

Uncoated MNPs	VSM diameter (nm)	σ	TEM diameter (nm)	σ	DLS diameter (nm)
4SCC			12.72	0.29	28.8
4SCSC			11.88	0.28	26
4SC9SC	9.8	0.24	11.17	0.24	26.5
5SC13SC	7.8	0.16	9.4	0.17	6.2
7SC3SC	8.5	0.2	9.99	0.2	16.7
8SCC	8.6	0.21	9.23	0.21	15.5

8SC4SC	7.36	0.22	8.54	0.22	11.6
8SC5SC	7.4	0.19	7.73	0.19	12
4SCS9C4SC			10.68	0.17	15.3
7SC12SC			7.61	0.18	9.9
6SC26SC			7.21	0.18	9.4
2SC31SC			12.14	0.35	
YP1416SC			5.6	0.25	7.8
YP1417SC			4.5	0.16	9.2
Coated MNPs	VSM diameter (nm)	σ	TEM diameter (nm)	σ	DLS diameter (nm)
4SCC-PAAMA			12.72	0.29	21.5
4SCSC-PAAMA			11.88	0.28	34.2
4SC9SC-PAAMA	9.8	0.24	11.17	0.24	34.7
5SC13SC-PAAMA	7.8	0.16	9.4	0.17	21.9
7SC3SC-PAAMA	8.5	0.2	9.99	0.2	22.6
8SCC-PAAMA	8.6	0.21	9.23	0.21	22
8SC4SC-PAAMA	7.36	0.22	8.54	0.22	20
8SC5SC-PAAMA	7.4	0.19	7.73	0.19	55.2
4SC9SC4SC-PAAMA			10.68	0.17	25.5
2SC31SC-PAAMA			12.14	0.35	
YP1416SC-PAAMA			5.6	0.25	15.5
YP1417SC-PAAMA			4.5	0.16	17.6

1
2
3
4 **NMR relaxivity on coated and non-coated size-sorted maghemite**
5 **nanoparticles**
6

7
8 *Jérôme Fresnais^{1*}, QianQian Ma¹, Linda Thai¹, Patrice Porion², Pierre*
9 *Levitz¹ and Anne-Laure Rollet^{1*}*
10

11
12
13 *¹ Sorbonne Université, CNRS, Laboratoire de Physico-chimie des Electrolytes et*
14 *Nanosystèmes Interfaciaux, PHENIX - UMR 8234, F-75252 Paris cedex 05, France.*
15

16
17 *² Interfaces, Confinement, Matériaux et Nanostructures, ICMN, UMR 7374,*
18 *CNRS - Université d'Orléans, 45071 Orléans Cedex 02, France*
19

20
21
22
23
24 * anne-laure.rollet@sorbonne-universite.fr ; jerome.fresnais@sorbonne-universite.fr
25
26
27
28
29
30
31
32
33
34
35
36
37
38
39
40
41
42
43
44
45
46
47
48
49
50
51
52
53
54
55
56
57
58
59
60

NMR relaxivity on coated and non-coated size-sorted maghemite nanoparticles

Relaxation dispersion profile, i.e. frequency dependence of the proton longitudinal relaxation times, were recorded for numerous samples of iron oxide nanoparticle dispersion with narrow size dispersity and diameters varying from 4 to 12.5 nm. We demonstrated that r_1 and r_2 NMR relaxivities increase with nanoparticle diameter, as expected by the models. We also analyze the role of polydispersity for nanoparticles with the same mean size on the dispersion curves. Then, we compared intensively the role of coating on nanoparticles NMR relaxivity between bare and poly(sodium acrylate-co-maleate) coated nanoparticles. At last, we investigated the influence of nanoparticle size on the activation energy E_a . Interestingly, while E_a decreases with nanoparticle diameter when determined from T_1 , it increases for T_2 determination. The influence is more important for small particles (<9 nm) than for big particles (>9 nm). More, the PAAMA coating changes the energy E_a obtained from T_2 : E_a becomes independent of the nanoparticle diameters.

Keywords: maghemite nanoparticles; polymer coating; NMR relaxivity

Introduction

The magnetic nanoparticles (MNPs) are widely studied and used for their high efficiency as contrast agent in MRI combined with their therapeutic properties¹⁻³. There are two major contributions to the relaxation of the magnetic moment of MNPs. First, their magnetic moment is proportional to the volume of the particles. The relaxation rates are thus largely ruled by the size of the particles, as well as by their anisotropy⁴. Second, the role of the coating on iron oxide nanoparticles is often neglected but can

1
2
3 drastically modify the MNPs relaxation process ^{5,6}. Indeed, the coating can contribute to
4 slow down the rotation of MNPs and modify the diffusion of solvent molecules
5 compared to the medium. The relaxivity properties r_1 and r_2 , i.e. the relaxation rate of
6 the surrounding nuclei R_1 and R_2 divided by the concentration of iron, are the two
7 parameters that are determined experimentally. They are usually obtained at a unique
8 frequency, but more informations can be obtained by their determination at various
9 frequencies ⁷. Experimental results highlight that r_1 and r_2 varies with nanoparticle
10 diameter ⁸. The particle with the optimal diameter is thus an important parameter to be
11 taken into account for bio-applications for magnetic resonance imaging (MRI) ⁷.
12 However, only few to no systematic experimental works were conducted to measure the
13 relaxivity of iron oxide nanoparticles on a large range of particle size with controlled
14 (and low) polydispersity. On the more, one important factor can impact the relaxivities
15 of water in presence of MNPs. Indeed, it has also been evidenced that the aggregation
16 state of the particle plays a crucial role in their relaxivity properties ⁹⁻¹¹. However, once
17 incorporated in living animals, the MNPs may agglomerate or simply not be in a bulky
18 state (adsorption on membrane cell...) ¹². Thus, the main recent developments are
19 devoted to the design of efficient coatings that avoid or at least reduce magnetic dipolar
20 interactions between MNPs ^{3,13}. Once again, the coating can modify significantly the
21 relaxation process by slowing the rotation of the particles and perturbing the diffusion
22 of solvent molecules in the vicinity of the MNPs.
23
24
25
26
27
28
29
30
31
32
33
34
35
36
37
38
39
40
41
42
43
44
45

46 Complementarily, the response depends on the nature of MNPs. The example of
47 maghemite and cobalt ferrite MNPs is illustrative. The magnetic anisotropy energy
48 constant K that reflects the way the magnetic moment of the MNPs fluctuates along the
49 easy magnetic axes, is very different in these two cases ¹⁴. For maghemite, its value is
50 quite low (about 6 kJ/mol) and is ruled by surface effects ^{15,16}. For cobalt ferrite, its
51
52
53
54
55
56
57
58
59
60

1
2
3 value is about 10 times higher than for maghemite and originate from the core of MNPs,
4
5 surface effects being negligible. Hence, adsorption of molecules on maghemite MNPs
6
7 might lead to important consequences on their relaxivity properties¹³. On the contrary,
8
9 the cobalt ferrite MNPs relaxivity properties should be much less affected by coating.
10

11
12
13 In this article, we have been interested in the maghemite MNPs. The study of relaxivity
14
15 properties is often hindered by polydispersity of MNPs batch that are produced and used
16
17 in classical studies. Herein we focus on a drastic size sorting process to obtain large
18
19 MNPs batches with controlled size and low polydispersity (less than 0.2, according to a
20
21 lognormal size distribution). We systematically compared the relaxivities of bare MNPs
22
23 and poly(acrylate-co-maleate) coated nanoparticles, and explored the activation energy
24
25 of uncoated and coated particles.
26
27

28 29 30 **Experimental and method**

31 32 33 *Maghemite nanoparticles synthesis and coating*

34
35 Iron oxide nanoparticles with bulk mass density $\rho = 5.10^3 \text{ kg.m}^{-3}$ were synthesized
36
37 according to the Massart's pathway by aqueous alkaline co-precipitation of iron (II) and
38
39 iron (III) salts and oxidation of the magnetite (Fe_3O_4) into maghemite ($\gamma\text{-Fe}_2\text{O}_3$) to
40
41 prevent further oxidation¹⁷. At pH = 1.8, the bare particles are positively charged, with
42
43 nitrate counter-ions. They have a diameter size distribution centered on 8 nm according
44
45 to a lognormal distribution. The resulting inter-particle interactions are repulsive and
46
47 impart an excellent colloidal stability to the dispersion. However, the nanoparticle
48
49 polydispersity is high (typically 0.45 following the lognormal distribution). As the
50
51 magnetic properties are proportional to the volume of the nanoparticles, the
52
53 polydispersity induce an average of the magnetic properties, thus the relaxivities. To
54
55
56
57
58
59
60

1
2
3 highlight more precisely the influence of size nanoparticles on relaxivity, a size sorting
4
5 has been achieved.

6
7 Size sorting is used to select sample with controlled size and lower size polydispersity.
8
9 A well-established method was followed to obtain different sample with narrow size
10
11 distribution ¹⁸. Electrostatic repulsion between nanoparticles can be screened by the
12
13 addition of salt. The repulsion will depend on the volume of the nanoparticles, and a
14
15 phase separation is obtained where the concentrated phase contains the largest particles
16
17 and the dilute one the smallest. Multiple steps of size sorting were achieved to obtain
18
19 samples with the narrowest size distribution ($\sigma < 0.2$) and diameters going from 4.5 nm
20
21 to 12 nm (see figure SI-1 for the size sorting pathway for the samples used in this
22
23 study).
24
25

26
27 Experimentally, a given volume of nitric acid is added to the ferrofluid, that is
28
29 placed on a magnet to separate the condensed phase (C) from the supernatant (S). The
30
31 dense phase is washed with acetone and diethyl ether and redispersed in water. Another
32
33 amount of nitric acid is added to the supernatant phase (S) and a second condensed
34
35 phase (SC) is recovered and washed to obtain a second sample. The protocol is
36
37 reproduced (samples 2SC, 3SC...) until the final supernatant is free from iron oxide
38
39 nanoparticles. If the polydispersity of each sample is too large, each sample is sorted
40
41 again by size following the same process. For instance, 5SC sorting processes give
42
43 samples which are named 5SC1SC, 5SC2SC...
44
45

46
47 Ferrofluids were characterized with Vibrating Sample Magnetization (VSM),
48
49 Transmission Electron Microscopy (TEM), atomic absorption spectrometry, and UV-
50
51 Visible spectrometry (see table 1 in SI-2 for complete informations about the samples
52
53 used in this study).
54
55
56
57
58
59
60

1
2
3 Bare nanoparticles were coated with poly(acrylic acid-co-maleic acid) polymer chains
4 (PAAMA) using electrostatic interactions between carboxylate functions and the
5 positive charges on the nanoparticles, similarly to a previous pathway used to coat
6 MNPs with poly(sodium acrylate)¹⁹. PAAMA was purchase at Sigma Aldrich and was
7 used without any purification. It consists of chains with average molecular weight of
8 3000 g/mol with a molar ratio 1:1 between each monomers. A solution at 0.5 %wt. of
9 bare nanoparticles is added to a 0.5%wt. of PAAMA (1:2 volume ratio) at acidic pH
10 value (1.8). A flocculation is induced by the interaction between the PAAMA and the
11 nanoparticles. The transparent supernatant is removed and the pH of the condensed
12 phase is increased up to 10 to redispersed the nanoparticles. This coating is particularly
13 efficient to stabilize the nanoparticles in brine or complex media²⁰.

Maghemite nanoparticles characterization

31
32 TEM is used to analyze physical size distribution of each nanoparticle sample. From
33 different images, diameters of nanoparticles are measured. A statistic is achieved to
34 obtain the size distribution of the nanoparticles. A lognormal distribution is used to fit
35 the experimental data and obtain a mean diameter and a size polydispersity. This size is
36 different from hydrodynamic diameter obtained by dynamic light scattering and the one
37 obtained by VSM. This diameter resulting from the TEM image analysis is used to
38 compare the relaxivity properties.

39
40
41
42
43
44
45
46
47
48
49 The concentration of ferrofluid are determined using both atomic absorption and UV-
50 visible spectroscopies²¹. Both methods lead to comparable results.

51
52
53
54
55
56
57
58
59
60
Magnetic properties were obtained from a homemade VSM at room temperature,
operating between -1 Tesla and +1 Tesla. From magnetization curves, magnetization at

1
2
3 saturation and magnetic susceptometry were obtained. These values are used to
4
5 modelize the relaxometry dispersion curves.

6
7 The measurements of the water ^1H relaxation times (T_1 and T_2) were carried out on four
8
9 different NMR apparatus. At 2 T (100 MHz for ^1H resonance frequency), the
10
11 experiments were carried out using DSX100 Bruker spectrometer equipped with a
12
13 diffusion probe (diff30 Bruker). The T_1 was measured using an inversion-recovery
14
15 sequence and T_2 using a Hahn echo, with 0.2s recycle delay. At 1.2 T (60MHz) and 0.4
16
17 T (20MHz), the experiments were carried out using a 60 and a 20 Bruker Minispec,
18
19 respectively. T_1 was measured using an inversion-recovery sequence with 16 recovery
20
21 delays ranging from 40 μs to 10 T_1 approximately. T_2 using a CPMG sequence with 50
22
23 to 500 echoes separated by 80 μs , a recycle delay of 0.2 s.

24
25
26 The low frequency domain from 10 kHz to 15 MHz is explored on a Stellar Spin
27
28 Master relaxometer. In this case, only T_1 has been measured using a PP sequence from
29
30 10 kHz to 8 MHz and a NP sequence from 8 MHz to 15 MHz²².

31
32
33 The relaxivities $r_1 = (T_1 [\text{Fe}])^{-1}$ and $r_2 = (T_2 [\text{Fe}])^{-1}$ were determined using five
34
35 MNPs dispersions with the iron concentration $[\text{Fe}]$ ranging from 0.5 to 20mM,
36
37 approximately. In this range, the relaxation rates $R_1 = 1/T_1$ and $R_2 = 1/T_2$ vary linearly
38
39 with $[\text{Fe}]$, and the r_1 and r_2 values are obtained with a linear regression (figure S1). On
40
41 the Stellar Spin Master, the measurements were performed for only one concentration
42
43 because of the duration of the experiments. At 0.47 T, the relaxivities r_1 and r_2 were
44
45 measured as a function of five different temperatures ($T=10, 17, 25, 33$ and 40°C).

50 51 **Results and discussion**

52
53
54
55
56
57
58
59
60

Effect of polydispersity

The size polydispersity of the nanoparticles dispersion has an obvious effect on relaxivity as the latter is influenced by nanoparticles size and shape. To illustrate this influence, the r_1 and r_2 at 20 MHz has been recorded for a large panel of maghemite samples and the r_1 profile has been recorded for two samples of the same medium size but with different polydispersity.

The polydispersity σ of our samples was determined from the analysis of TEM images using ImageJ software and fitted using a log-normal function fitted over several thousand of MNPs.

$$f(x; \mu, \sigma) = \frac{1}{x\sigma\sqrt{2\pi}} \exp\left(-\frac{(\ln x - \mu)^2}{2\sigma^2}\right)$$

The effect of polydispersity is first presented at one Larmor frequency (20 MHz) in order to show its effect depending on the MNPs size. Figure 3 shows the value of r_1 and r_2 as a function of the MNPs size for several set of samples with different polydispersity: $\sigma < 0.2$, $\sigma \approx 0.24$, $\sigma \approx 0.3$, $\sigma \approx 0.35$, and $\sigma > 0.4$.

With no surprise, the greater size polydispersity, the greater r_1 and r_2 value dispersion. The effect is much more pronounced for r_1 than for r_2 , for which the all points are relatively grouped. It can also be noticed that the increase of the polydispersity leads to lower relaxivity values for a given medium size. At first sight, it seems surprising because the increase of σ in the log-normal function for a given medium size implies that the proportion of bigger MNPs is higher in the sample and an increase of the MNPs size leads to higher r_1 and r_2 relaxivities as shown in the same figure 3.

In order to clarify this phenomenon, we have recorded the relaxation dispersion curve for two samples of the same medium size but with very different polydispersity: $d_0 = 10.8$ nm with $\sigma = 0.17$ and $\sigma = 0.53$ i.e. non sorted sample (figure 4). For the

1
2
3 maghemite sample with low polydispersity, the curve presents a well-defined profile
4
5 with a plateau at low frequency, a depression just before the peak around 7 MHz and the
6
7 decrease at high frequency. For the maghemite sample with large polydispersity, the
8
9 characteristic figure of maghemite dispersion profile is shaded. The depression before
10
11 the peak has disappeared and the peak is somehow crushed, i.e. broader and less
12
13 intense. Moreover, its position is shifted toward low frequency. Hence, it can also be
14
15 noticed that at high frequency, i.e. around 20 MHz, it leads to a lower r_1 value as
16
17 compared to the sample with low polydispersity.
18
19
20

21 *Effect of size*

22
23 We now present only the results for the highly sorted samples, i.e. for which the
24
25 polydispersity is lower than 0.2. Their NMR relaxivities r_1 et r_2 are plotted as a function
26
27 of the TEM diameter in figure 5. An important increase is observed for both the
28
29 longitudinal and the transversal components. The slope are about $6.4 \text{ s}^{-1} \text{ mM}^{-1}$ per nm
30
31 for r_1 and $17.8 \text{ s}^{-1} \text{ mM}^{-1}$ per nm for r_2 . This difference is due to the dependence of the
32
33 difference in the Curie term for r_1 and for r_2 .
34
35

36 Our values are well in line with the huge compilation study of Vuong et al. ⁷
37
38 where the variation of r_2 with the size of MNPs has been studied over a very wide range
39
40 of size (using also aggregates of MNPs). The authors show the linear dependence of
41
42 r_2/M_v with the particle diameter where M_v is the saturation magnetization and this
43
44 dependence pertains up to $0.4 \mu\text{m}$.
45
46

47 The effect of size on r_1 is not usually studied because the targeted application for
48
49 MNPs is T_2 contrast agent. r_1 continuously increases with the diameter and tends to be
50
51 linear in this range of size. This variation differs from the one observed for MNPs with
52
53 high magnetic anisotropy constant like cobalt ferrite MNPs. In the latter case, r_1
54
55 increases with MNPs size but the slope decreases with the diameter.
56
57
58
59
60

1
2
3
4
5 Tabletop relaxometer allows us to record rapidly the r_1 and r_2 and ergo to be
6
7 able to study a lot of samples relaxivities. Considering the data discrepancies in the
8
9 literature, it is crucial to get statistics to investigate parameters like size, coating etc.
10
11 This is an obvious advantage of this kind of relaxometers. However, the effect of the
12
13 various parameters is better revealed by NMR relaxation profile.
14

15
16 On figure 6 are presented the r_1 profiles for non-coated MNPs with ($\sigma \leq 0.2$) and
17
18 with diameter ranging from 4 to 11 nm. By increasing the size of spherical
19
20 superparamagnetic nanoparticles several features occurs in the r_1 profile: (a) the
21
22 maximum of the bump is shifted toward lower frequency, (b) the height of this
23
24 maximum is increased, (c) the value of the plateau at low frequency is increased and (d)
25
26 the hollow just before the bump is decreased. As already explained by Roch et al.²³ in
27
28 their model, these variations are the result of a balance between the different dynamical
29
30 characteristic times of the system (Neel time, diffusion time, rotational time).
31
32
33
34
35
36

37 ***Effect of coating***

38 The PAAMA coating is achieved through electrostatic anchoring of the
39
40 carboxylate functions at the nanoparticle surfaces. The molecular weight of the
41
42 PAAMA chains (3,000 g/mol) corresponds to qualitatively 16 equivalent monomers of
43
44 acrylate-maleate. This corresponds to a total length of the polymer chain of qualitatively
45
46 10-12 nm when completely elongated. Part of the monomers is adsorbed on the surface
47
48 of the nanoparticles, and the chains are not completely straight in solution. This reduced
49
50 drastically the thickness of the PAAMA corona around nanoparticles. Dynamic light
51
52 scattering experiment comparing bare and PAAMA coated MNPs demonstrated an
53
54
55
56
57
58
59
60

1
2
3 increase of diameter of 4-5 nm for almost all MNPs batches, that is in good agreement
4
5 with what was observed for poly(sodium acrylate) coated nanoparticles²⁴.
6

7 Bare and PAAMA coated MNPs were characterized by VSM. Curves between
8
9 uncoated and coated MNPs are superimposed, and give same diameters and
10
11 polydispersities before and after coating. This shows that the coating has no influence of
12
13 the magnetic behavior of MNPs against applied magnetic field.
14

15
16 The values of r_1 and r_2 for PAAMA coated MNPs at 20 MHz are compared with
17
18 those of non-coated MNPs (figure 5). The diameter considered here is the maghemite
19
20 diameter without the polymer corona. The values are clearly superimposed for the r_2
21
22 while for the r_1 for PAAMA coated MNPs are slightly below the r_1 for non-coated
23
24 MNPs. It can be noted that the effect of coating on the r_1 and r_2 at high frequency is
25
26 subject to high discrepancies of partially and uncontrolled MNPs aggregation
27
28 phenomena²⁵. Hence, the r_1 profiles is more able to reveal the coating effect.
29

30
31 The r_1 profiles have been recorded for PAAMA coated MNPs and plotted in
32
33 figure 6. The evolution of the curves with the MNPs diameter is very similar to the
34
35 curves for non-coated MNPs. In order to better reveal the effect of the PAAMA coating,
36
37 the profile for non-coated and PAAMA coated MNPs have been superimposed for four
38
39 sizes, 5.6, 7.7, 10.0 and 12.7 nm in figure 7. Several observations can be made when the
40
41 MNPs are coated: (a) the value of the plateau at low frequency is smaller; (b) the hollow
42
43 before the bump is less pronounced; (c) the position of the hollow is shifted toward low
44
45 frequency; (d) the position of the bump is not shifted; (e) the bump maximum is
46
47 affected and (f) the profiles tend to merge at high frequency.
48
49
50
51

52 To illustrate these effects, we have also plotted in figure 8 the ratio A between
53
54 the maximum of r_1 (r_1^{\max}) and the r_1 at 10 kHz (the plateau value r_1^{plateau}) and the ratio B
55
56
57
58
59
60

1
2
3 between the minimum of r_I before the bump (r_I^{deep}) and the r_I^{plateau} . From figure 8 it is
4 clear that the height associated to the Curie term in the models²⁶ is increased with the
5 coating. It can be also notice that the difference between the ratio A for non-coated and
6 coated MNPs is roughly constant with the maghemite diameter. The striking point is
7 that the position of the bump is not affected in the same time. The models predict a
8 combined modification of the bump height and its position^{14,23}. As illustrated by Kruk
9 et al.²⁷ in maghemite MNPs dispersed in decaline and in toluene, a slowdown of the
10 solvent dynamics lead to both the decrease of the bump and the shift of its position
11 toward low frequencies. In the latter case, two solvents of different viscosities were
12 used. In the case of coated MNPs, only the dynamics of water inside the polymer corona
13 and in the very close vicinity is modified (along with the dynamics of the whole MNPs).
14 To modelize the relaxivity of polymer coated MNPs it is therefore necessary to
15 reconsider the diffusion propagator of water with a two steps environments. On figure 8,
16 we have also plotted the ratio B between the minimum of r_I before the bump (r_I^{deep}) and
17 the r_I^{plateau} . Here again a clear feature can be observed.

18
19
20
21
22
23
24
25
26
27
28
29
30
31
32
33
34
35
36
37
38
39
40 The MNPs in the models are impenetrable sphere and the diffusion of water is
41 homogenous whatever the distance to the MNPs. In the case of polymer coated MNPs
42 there is a corona around the MNPs where the diffusion of water is hindered. The effect
43 of the modification of water diffusion in the vicinity of MNPs has been underlined by
44 Ye et al.²⁸ who compared the relaxivities of magnetite coated by silica or capped by
45 cetyltrimethyl ammonium bromide.
46
47
48
49
50
51
52
53
54
55
56
57
58
59
60

Activation energy

The relaxivity r_1 and r_2 at 20 MHz have been measured at different temperatures ranging from 10 to 40°C. In this range, the relaxivities exhibit an Arrhenius behavior and it was possible to determine an activation energy E_a . It must be underlined that at 20 MHz the relaxivity is ruled by the Curie term. The latter is related to the characteristic time $\tau_D = d^2/D$ of the water diffusion around the MNPs (d is the diameter of the MNPs and D is the self-diffusion coefficient of water). The energy E_a values obtained are in the same range of E_a for bulk water (19 kJ/mol)²⁹. The results are presented in figure 9 as function of the maghemite size. For the non-coated MNPs, the first striking point is the difference of behaviour in the E_a variations for r_1 and for r_2 . For r_1 E_a is constant for small MNPs approximately up to 10nm, and then decreases. The behavior is opposite for r_2 E_a as the latter increases up to 10 nm and then is roughly constant. It must be stressed also that these variations are very different from those observed for MNPs with high magnetic anisotropy. In the case of cobalt ferrite MNPs E_a of both the r_1 and the r_2 decreases. These differences are very interesting because MNPs with high (cobalt ferrite) and low (maghemite) magnetic anisotropy energy have very different r_1 profiles, but above 20 MHz, their r_1 and r_2 values are very similar. Therefore, the only measurement of E_a for r_1 and the r_2 relaxivities using a tabletop relaxometer is not sufficient to investigate the magnetic anisotropy effects. The measurement of E_a of r_1 and r_2 thus opens an opportunity for such studies and furthermore for studies on the tuning of the anisotropy properties.

The coating influences slightly the r_1 and the r_2 activation energy. For small size MNPs, E_a is increased by the coating while no effect is observed for larger maghemite (>8 nm). Greater effect was expected as the E_a , at this frequency, is dominated by the Curie term,

1
2
3 i.e. correlated with the τ_D time. Hence the polymer corona seems to affect the
4
5 relaxivities properties only for small maghemite MNPs.
6
7

8
9 To analyze more precisely the impact of the coating on the activation energy, we can
10
11 evaluate the role of surface to volume ratio, that is proportional to the inverse of the
12
13 particle diameter. Indeed, we should be able to highlight the role of the coating on the
14
15 relaxation process. Thus, we plotted the ratio between activation energies E_a (measure
16
17 either on T_1 or T_2) of coated and uncoated particles versus the inverse of the particles
18
19 diameter (figure 10).
20
21
22
23

24
25 There are clearly some dispersions in measurements, but it can be seen that the
26
27 activation energy ratio measured on T_1 values are mainly larger than unity, and
28
29 increases with the inverse of the diameter. The activation energy ratio values obtained
30
31 from T_2 measurement shows an increase with increasing value of $1/D$ as well, as
32
33 observed with E_a values measured from T_1 . These results show that the coating on the
34
35 nanoparticles play a significant role in the relaxation process of water molecules in the
36
37 polymer corona compared to bare MNPs.
38
39

40 **Conclusion**

41
42 The influences of the size, the sample polydispersity and the polymer coating of
43
44 maghemite nanoparticles on NMR relaxivities have been investigated. In agreement
45
46 with previous studies, r_1 and r_2 increase with the MNPs diameter. The NMR relaxation
47
48 profile better reveal the influence of the size with a shift of the r_1 maximum toward low
49
50 frequency. It is shown the importance of controlling the size of the sample as in addition
51
52 to higher discrepancy in r_1 and r_2 values, the NMR relaxation profile is significantly
53
54 changed with a general broadening and an important shift of the r_1 maximum toward
55
56
57
58
59

low frequency. Polymer coating influences the relaxivities of maghemite MNPs as shown by the NMR relaxation profiles. The most striking and surprising feature is that the height of the bump is modified while its position is unchanged. The activation energy of T_1 and T_2 have been measured at 20 MHz for non-coated and coated maghemite MNPs. This activation energy E_a exhibits an interesting dependence on the magnetic properties as its variation with MNPs size is clearly different for maghemite and cobalt ferrite MNPs, which magnetic anisotropy energy is ten times higher in the latter case than in the former case. The E_a of maghemite MNPs is influenced by the polymer coating only for small size MNPs (<8 nm).

Acknowledgement

The authors acknowledge COST Action **CA15209 EURELAX "European Network on NMR Relaxometry"**, supported by COST (European Cooperation in Science and Technology).

References

- ¹ G. Béalle, R. Di Corato, J. Kolosnjaj-Tabi, V. Dupuis, O. Clément, F. Gazeau, C. Wilhelm, and C. Ménager, *Langmuir* **28**, 11834 (2012).
- ² S.A. Corr, S.J. Byrne, R. Tekoriute, C.J. Meledandri, D.F. Brougham, M. Lynch, C. Kerskens, L. O'Dwyer, and Y.K. Gun'ko, *J. Am. Chem. Soc.* **130**, 4214 (2008).
- ³ A.K. Gupta and M. Gupta, *Biomaterials* **26**, 3995 (2005).
- ⁴ A.-L. Rollet, S. Neveu, P. Porion, V. Dupuis, N. Cherrak, and P. Levitz, *Phys. Chem. Chem. Phys.* **18**, 32981 (2016).
- ⁵ S. Kachbi-Khelfallah, M. Monteil, M. Cortes-Clerget, E. Migianu-Griffoni, J.-L. Pirat, O. Gager, J. Deschamp, and M. Lecouvey, *Beilstein Journal of Organic Chemistry* **12**,

1
2
3 1366 (2016).

4
5 ⁶ E. Umut, in *Modern Surface Engineering Treatments*, edited by M. Aliofkhaezai
6
7 (InTech, 2013).

8
9
10 ⁷ Q.L. Vuong, J.-F. Berret, J. Fresnais, Y. Gossuin, and O. Sandre, *Advanced*
11
12 *Healthcare Materials* **1**, 502 (2012).

13
14 ⁸ M.-S. Martina, J.-P. Fortin, C. Ménager, O. Clément, G. Barratt, C. Grabielle-
15
16 Madelmont, F. Gazeau, V. Cabuil, and S. Lesieur, *J. Am. Chem. Soc.* **127**, 10676
17
18 (2005).

19
20 ⁹ I.Y. Tóth, D. Nesztor, L. Novák, E. Illés, M. Szekeres, T. Szabó, and E. Tombácz,
21
22 *Journal of Magnetism and Magnetic Materials* **427**, 280 (2017).

23
24 ¹⁰ E. Peng, F. Wang, and J.M. Xue, *J. Mater. Chem. B* **3**, 2241 (2015).

25
26 ¹¹ B.A. Larsen, M.A. Haag, N.J. Serkova, K.R. Shroyer, and C.R. Stoldt,
27
28 *Nanotechnology* **19**, 7 (2008).

29
30
31 ¹² R. Di Corato, A. Espinosa, L. Lartigue, M. Tharaud, S. Chat, T. Pellegrino, C.
32
33 Ménager, F. Gazeau, and C. Wilhelm, *Biomaterials* **35**, 6400 (2014).

34
35 ¹³ L.E.W. LaConte, N. Nitin, O. Zurkiya, D. Caruntu, C.J. O'Connor, X. Hu, and G.
36
37 Bao, *Journal of Magnetic Resonance Imaging* **26**, 1634 (2007).

38
39 ¹⁴ A. Rollet, S. Neveu, P. Porion, V. Dupuis, N. Cherrak, and P. Levitz, *Physical*
40
41 *Chemistry Chemical Physics: PCCP* (2016).

42
43
44 ¹⁵ C. Guibert, J. Fresnais, V. Peyre, and V. Dupuis, *Journal of Magnetism and Magnetic*
45
46 *Materials* **421**, 384 (2017).

47
48 ¹⁶ F. Gazeau, J.C. Bacri, F. Gendron, R. Perzynski, Y.L. Raikher, V.I. Stepanov, and E.
49
50 Dubois, *Journal of Magnetism and Magnetic Materials* **13** (1998).

51
52 ¹⁷ R. Massart and V. Cabuil, *Journal De Chimie Physique Et De Physico-Chimie*
53
54 *Biologique* **84**, 967 (1987).

- 1
2
3 ¹⁸ S. Lefebure, E. Dubois, V. Cabuil, S. Neveu, and R. Massart, *Journal of Materials*
4
5 *Research* **13**, 2975 (1998).
6
7 ¹⁹ A. Sehgal, Y. Lalatonne, J.F. Berret, and M. Morvan, *Langmuir* **21**, 9359 (2005).
8
9 ²⁰ C. Guibert, V. Dupuis, V. Peyre, and J. Fresnais, *J. Phys. Chem. C* **119**, 28148
10
11 (2015).
12
13 ²¹ C. Guibert, V. Dupuis, J. Fresnais, and V. Peyre, *Journal of Colloid and Interface*
14
15 *Science* **454**, 105 (2015).
16
17 ²² E. Anoardo, G. Galli, and G. Ferrante, *Applied Magnetic Resonance* **20**, 365 (2001).
18
19 ²³ A. Roch, R.N. Muller, and P. Gillis, *The Journal of Chemical Physics* **110**, 5403
20
21 (1999).
22
23 ²⁴ J. Fresnais, M. Yan, J. Courtois, T. Bostelmann, A. Bée, and J.-F. Berret, *Journal of*
24
25 *Colloid and Interface Science* **395**, 24 (2013).
26
27 ²⁵ Matthew R J Carroll and Phillip P Huffstetler and William C Miles and Jonathon D
28
29 Goff and Richey M Davis and Judy S Riffle and Michael J House and Robert C
30
31 Woodward and Timothy G St Pierre, *Nanotechnology* **22**, 325702 (2011).
32
33 ²⁶ M. Lévy, F. Gazeau, C. Wilhelm, S. Neveu, M. Devaud, and P. Levitz, *J. Phys.*
34
35 *Chem. C* **117**, 15369 (2013).
36
37 ²⁷ D. Kruk, A. Korpała, S.M. Taheri, A. Kozłowski, S. Förster, and E.A. Rössler, *The*
38
39 *Journal of Chemical Physics* **140**, 174504 (2014).
40
41 ²⁸ Ye Fei, Laurent Sophie, Fornara Andrea, Astolfi Laura, Qin Jian, Roch Alain, Martini
42
43 Alessandro, Toprak Muhammet S., Muller Robert N., and Muhammed Mamoun,
44
45 *Contrast Media & Molecular Imaging* **7**, 460 (2012).
46
47
48
49 ²⁹ J.H. Simpson and H.Y. Carr, *Phys. Rev.* **111**, 1201 (1958).
50
51
52
53
54
55
56
57
58
59
60

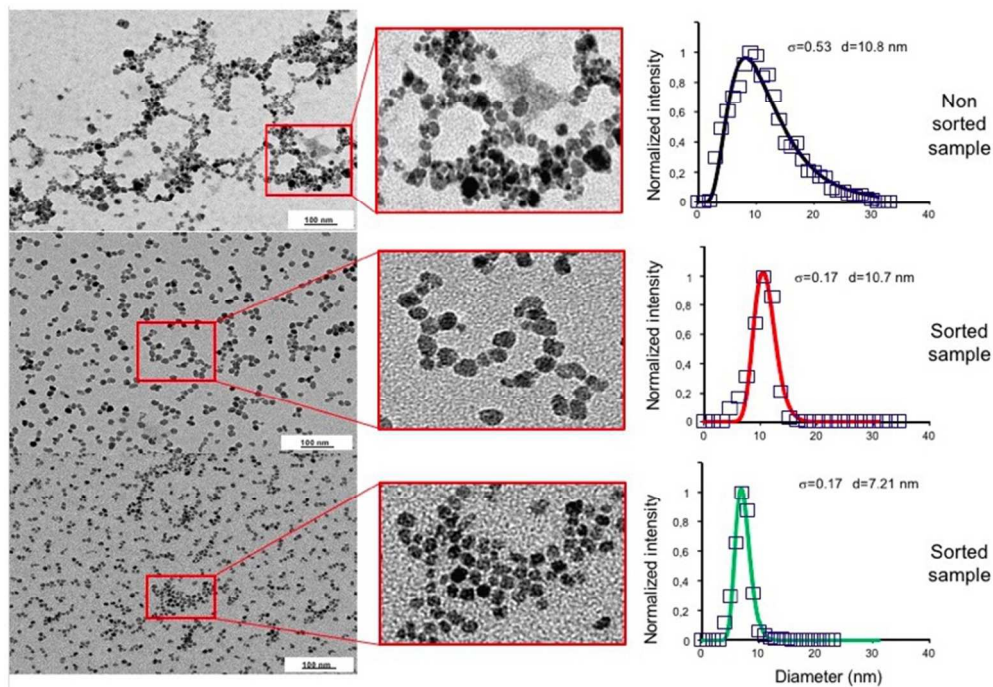


Figure 1: TEM image of the bare maghemite nanoparticles before sorting and after sorting process.

300x207mm (72 x 72 DPI)

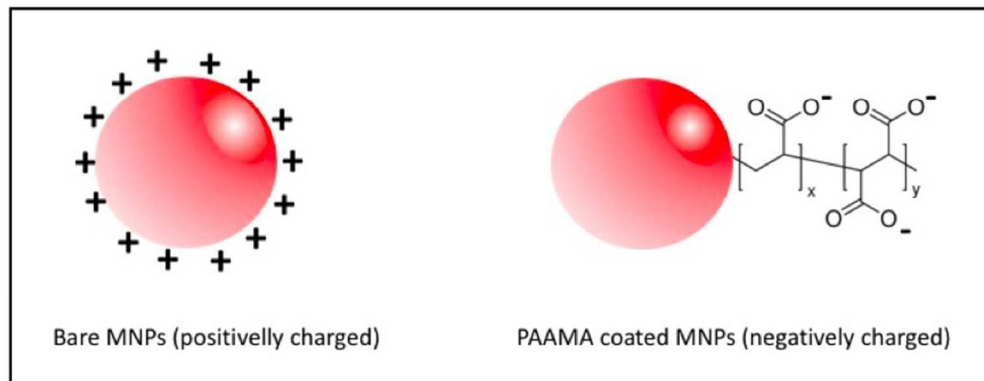


Figure 2: scheme of the bare maghemite nanoparticles (left) and PAAMA coated MNPs (right).

309x120mm (72 x 72 DPI)

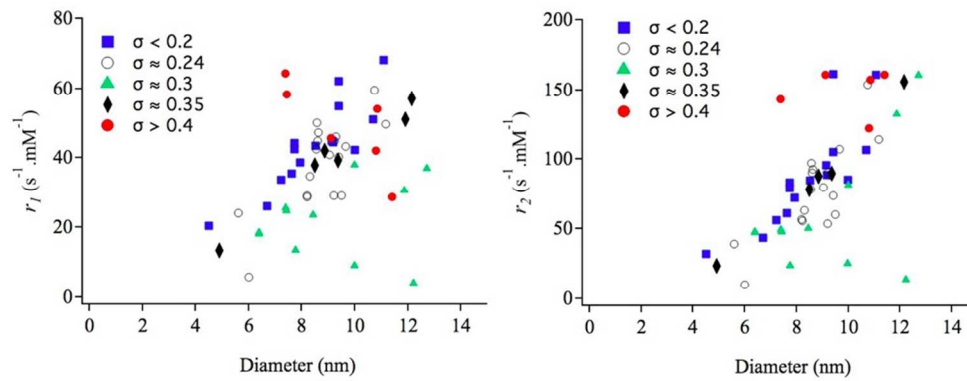


Figure 3: effect of the polydispersity σ on r_1 and r_2 : $\sigma < 0.2$ (blue squares), $\sigma \approx 0.24$ (empty circles), $\sigma \approx 0.3$ (green triangles), $\sigma \approx 0.35$ (black diamonds), and $\sigma > 0.4$ (red disks).

366x141mm (72 x 72 DPI)

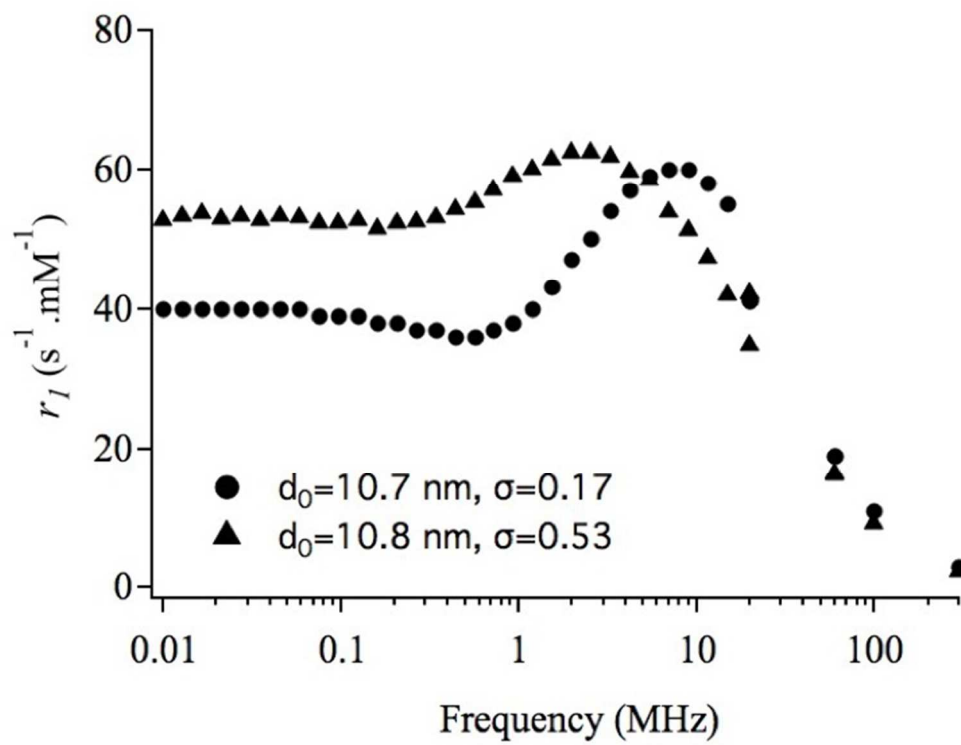


Figure 4: r_1 NMRD profile for two samples of the same medium size but with very different polydispersity: $d = 10.7 \text{ nm}$ with $\sigma = 0.17$ (circle) and $d = 10.8 \text{ nm}$ $\sigma = 0.53$ (triangle).

262x201mm (72 x 72 DPI)

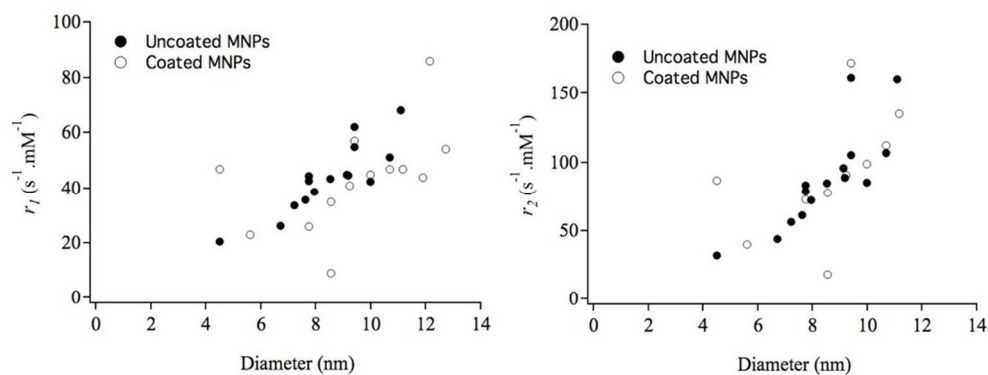


Figure 5: r_1 and r_2 relaxivities of uncoated (black symbol) and coated (empty symbol) maghemite as a function of the diameter (for $\sigma \leq 0.2$).

367x149mm (72 x 72 DPI)

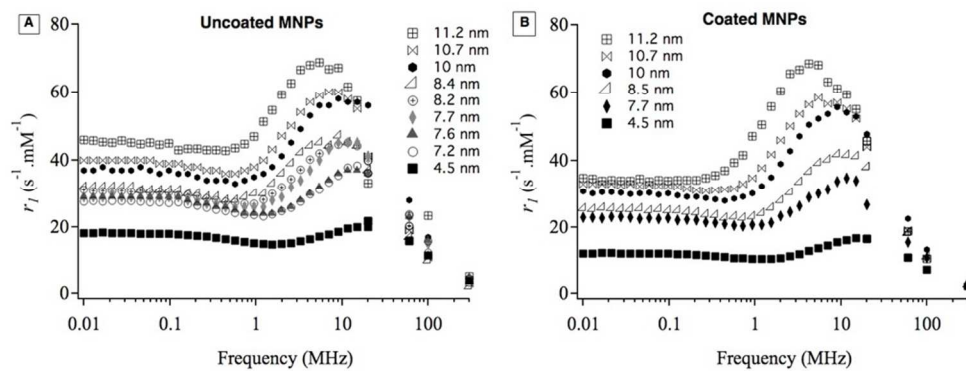


Figure 6: r_1 profile of maghemite uncoated MNPs (A) and PAAMA-coated MNPs (B) for diameters of the maghemite core (polymer corona not included) ranging from 4.5 to 11.2 nm.

368x141mm (72 x 72 DPI)

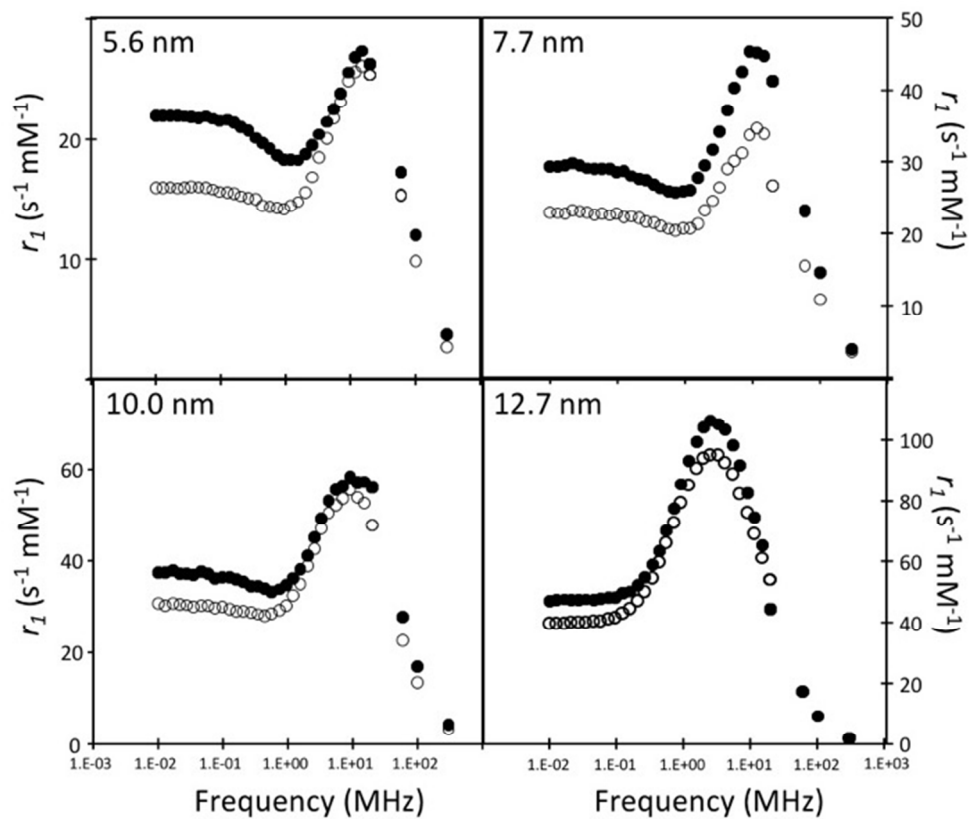


Figure 7: r_1 profile of maghemite MNPs non coated (black symbol) and PAAMA coated (empty symbol) for several diameters of the maghemite core (polymer corona not included): 5.6, 7.7, 10 and 12.7 nm.

254x213mm (72 x 72 DPI)

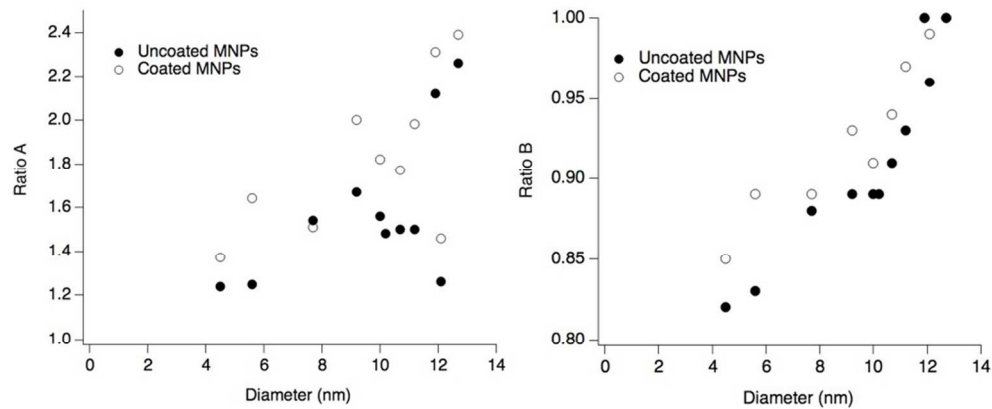


Figure 8: ratio A between the maximum of r_1 (r_{1max}) and the r_1 at 10 kHz (the plateau value $r_{1plateau}$) and the ratio B between the minimum of r_1 before the bump (r_{1deep}) and the $r_{1plateau}$ as a function of the maghemite diameter for uncoated (black disks) and coated (empty circles) MNPs.

361x155mm (72 x 72 DPI)

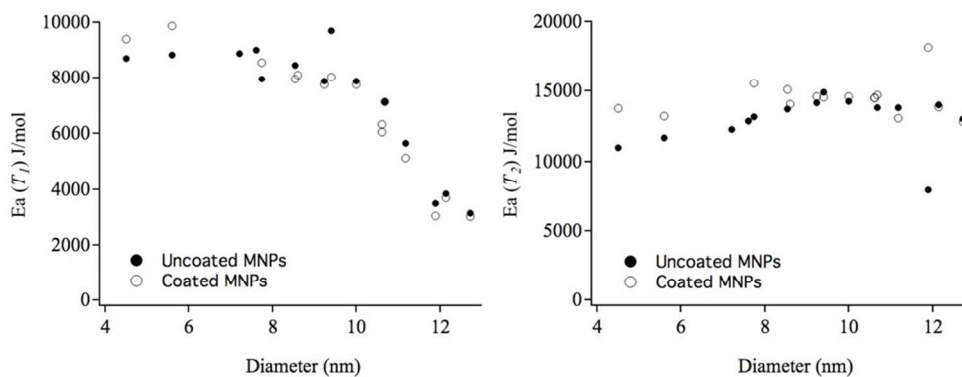


Figure 9: Activation energy E_a of T1 (left) and T2 (right) E_a for non-coated (black symbol) and coated (empty symbol) maghemite as a function of the diameter.

368x147mm (72 x 72 DPI)

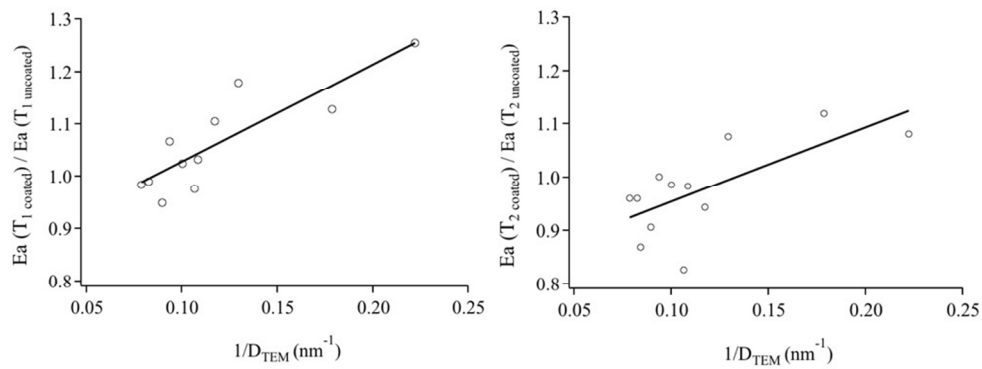


Figure 10: ratio of activation energy E_a of T1 (left) and T2 (right) E_a between non-coated and coated maghemite as a function of the inverse of the diameter. Lines are linear fits.

366x143mm (72 x 72 DPI)

NMR relaxivity on coated and non-coated size-sorted maghemite nanoparticles

Jérôme Fresnais^{1*}, QianQian Ma¹, Linda Thai¹, Patrice Porion², Pierre Levitz¹
and Anne-Laure Rollet^{1*}

¹ Sorbonne Université, CNRS, Laboratoire de Physico-chimie des Electrolytes et Nanosystèmes Interfaciaux, PHENIX - UMR 8234, F-75252 Paris cedex 05, France.

² Interfaces, Confinement, Matériaux et Nanostructures, ICMN, UMR 7374, CNRS - Université d'Orléans, 45071 Orléans Cedex 02, France

* anne-laure.rollet@sorbonne-universite.fr ; jerome.fresnais@sorbonne-universite.fr

Figures

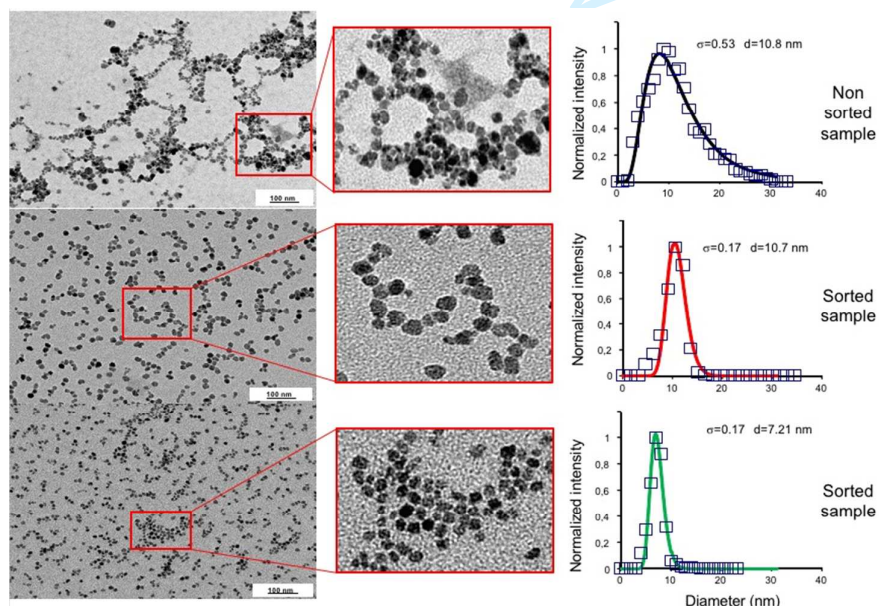


Figure 1: TEM image of the bare maghemite nanoparticles before sorting and after sorting process.

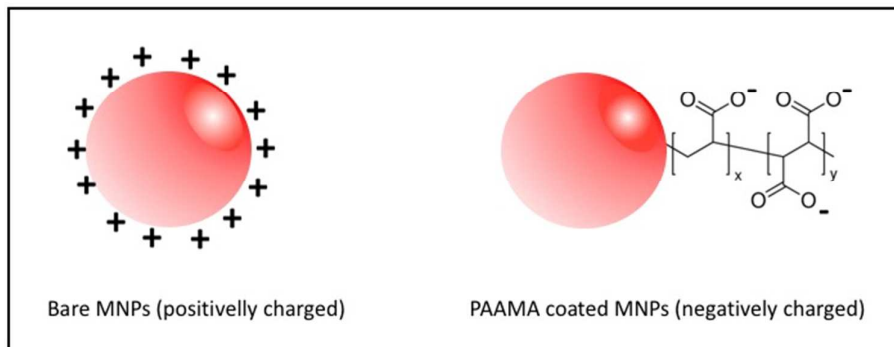


Figure 2: scheme of the bare maghemite nanoparticles (left) and PAAMA coated MNPs (right).

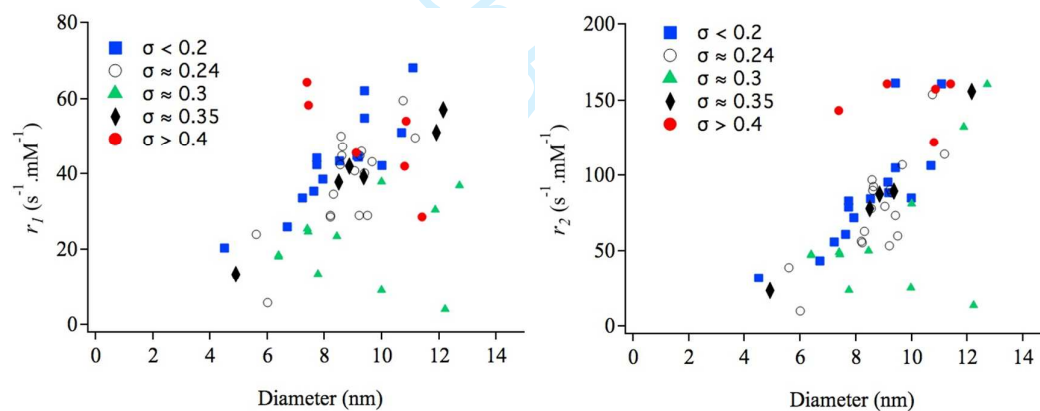


Figure 3: effect of the polydispersity σ on r_1 and r_2 : $\sigma < 0.2$ (blue squares), $\sigma \approx 0.24$ (empty circles), $\sigma \approx 0.3$ (green triangles), $\sigma \approx 0.35$ (black diamonds), and $\sigma > 0.4$ (red disks).

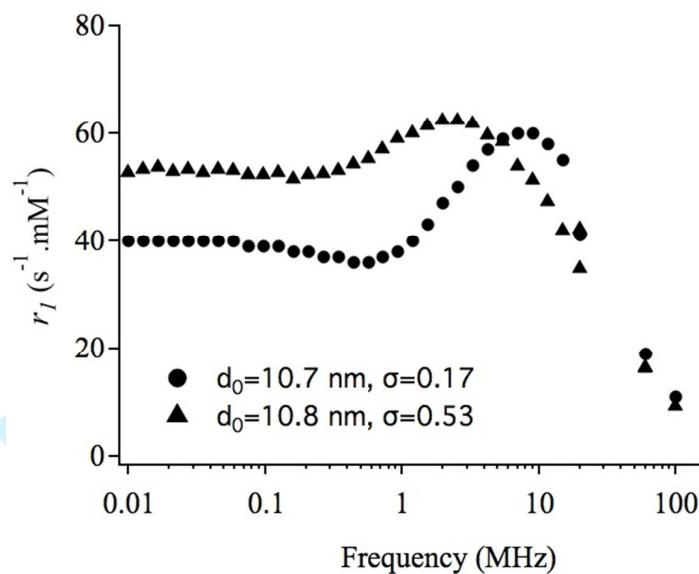


Figure 4: r_1 NMRD profile for two samples of the same medium size but with very different polydispersity: $d = 10.7$ nm with $\sigma = 0.17$ (circle) and $d = 10.8$ nm $\sigma = 0.53$ (triangle).

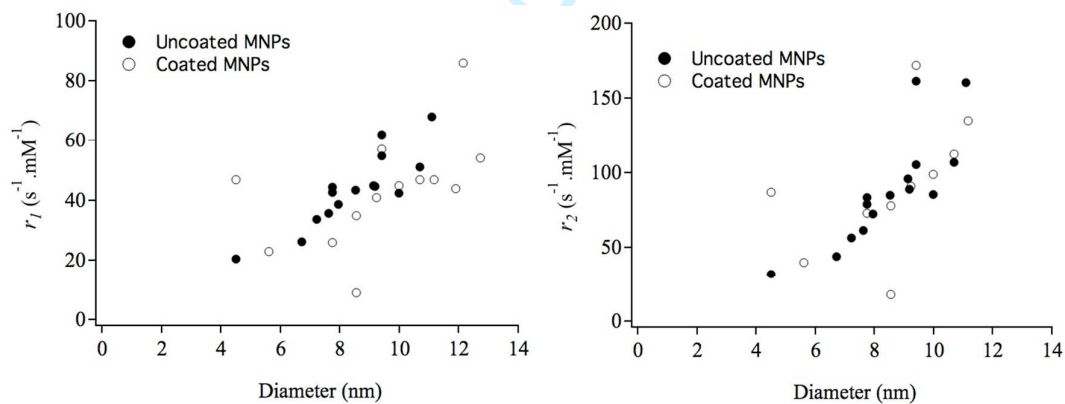


Figure 5: r_1 and r_2 relaxivities of uncoated (black symbol) and coated (empty symbol) maghemite as a function of the diameter (for $\sigma \leq 0.2$).

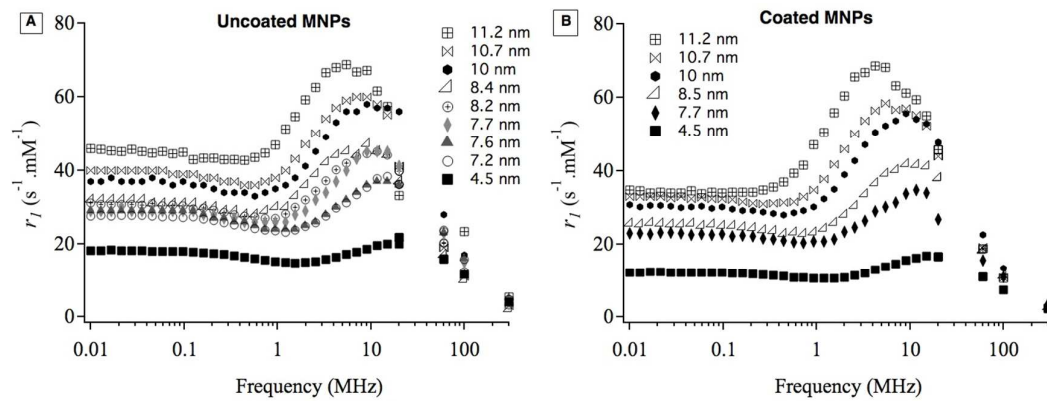


Figure 6: r_1 profile of maghemite uncoated MNPs (A) and PAAMA-coated MNPs (B) for diameters of the maghemite core (polymer corona not included) ranging from 4.5 to 11.2 nm.

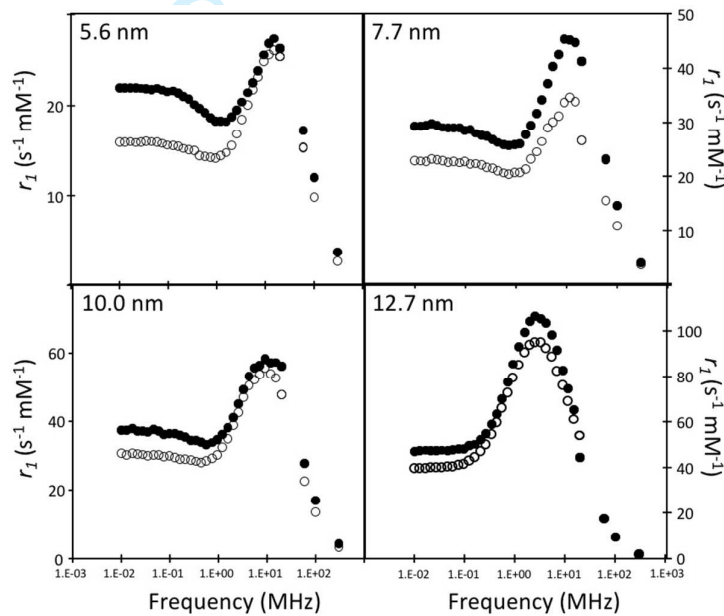


Figure 7: r_1 profile of maghemite MNPs non coated (black symbol) and PAAMA coated (empty symbol) for several diameters of the maghemite core (polymer corona not included): 5.6, 7.7, 10 and 12.7 nm.

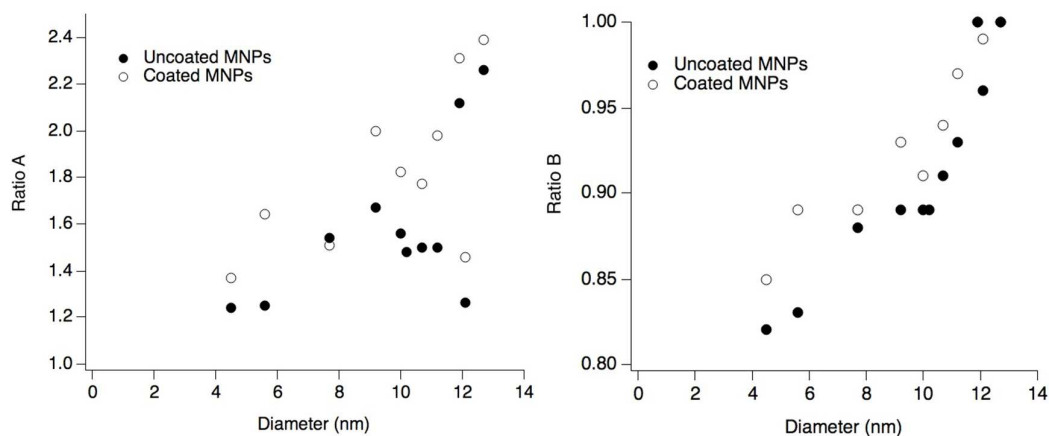


Figure 8: ratio A between the maximum of r_I (r_I^{\max}) and the r_I at 10 kHz (the plateau value r_I^{plateau}) and the ratio B between the minimum of r_I before the bump (r_I^{deep}) and the r_I^{plateau} as a function of the maghemite diameter for uncoated (black disks) and coated (empty circles) MNPs.

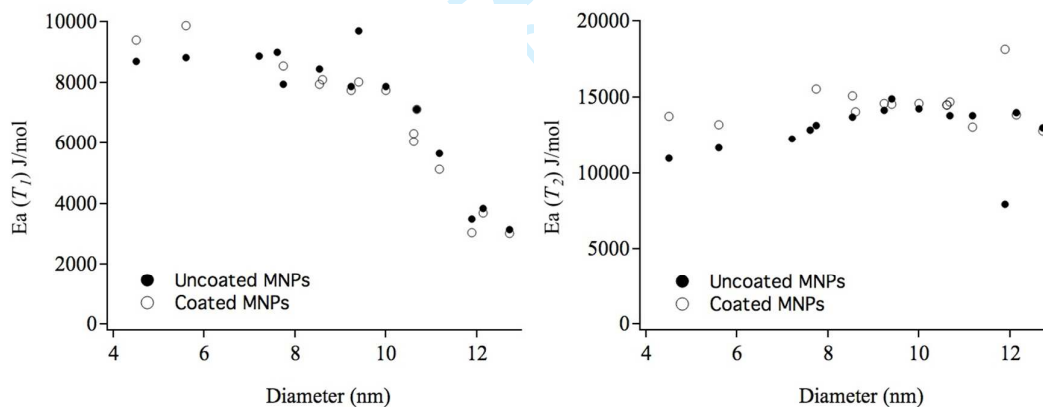


Figure 9: Activation energy E_a of T_1 (left) and T_2 (right) E_a for non-coated (black symbol) and coated (empty symbol) maghemite as a function of the diameter.

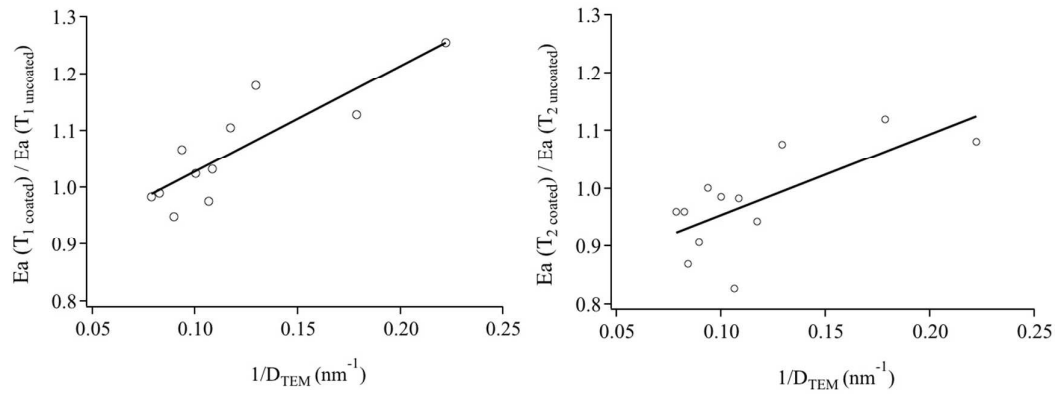


Figure 10: ratio of activation energy E_a of T_1 (left) and T_2 (right) E_a between non-coated and coated maghemite as a function of the inverse of the diameter. Lines are linear fits.